

Article

The Mechanism of *Elizabethkingia miricola* Infection of the Black Spotted Frog as Revealed by Multi-Omics Analysis

Qingcong Wei ^{1,†}, Dan Wang ^{2,†}, Kaijin Wei ², Bin Xu ² and Jin Xu ^{2,*}

¹ College of Fisheries and Life Science, Shanghai Ocean University, Shanghai 201306, China; weiqingcong@foxmail.com

² Yangtze River Fisheries Research Institute, Chinese Academy of Fishery Sciences, Wuhan 430223, China; wangdan@yfi.ac.cn (D.W.); weikj@yfi.ac.cn (K.W.); xubin@yfi.ac.cn (B.X.)

* Correspondence: xujin@yfi.ac.cn

† These authors contributed equally to this work and share first authorship.

Abstract: *Elizabethkingia miricola* (*E. miricola*) is a significant pathogen that causes the crooked head disease in black spotted frogs. This disease has plagued numerous frog farms in China and has resulted in substantial losses to the frog farming industry. Nonetheless, the exact mechanism that causes the disease in frogs remains unknown. In this study, transcriptomic and microbiomic analyses were conducted to analyze frog samples infected with *E. miricola* to reveal the infection mechanism of the pathogen. Liver transcriptomic analysis indicated that the livers of infected frogs had 1469 differentially expressed genes when compared with an uninfected group. These DEGs are mainly involved in immunity and metabolism, including neutrophil extracellular trap formation, the NOD-like receptor signaling pathway, leukocyte transendothelial migration, chemokine signaling pathway, Fc gamma R-mediated phagocytosis, and “metabolism”-related pathways such as the pentose phosphate pathway, carbon metabolism, glycerophospholipid metabolism, and glycerolipid metabolism. Similarly, 4737 DEGs were found in the kidney of infected frogs. These DEGs are mainly involved in immunity, including neutrophil extracellular trap formation, the NOD-like receptor signaling pathway, B cell receptor signaling pathway, C-type lectin receptor signaling pathway, complement and coagulation cascade, and Toll-like receptor signaling pathway. Ten immune-associated DEGs were screened in liver and kidney DEGs, respectively. And it was hypothesized that *E. miricola* infection could influence the host immune response. Microbiome analysis results showed that some opportunistic pathogens such as *Citrobacter*, *Shigella*, and *Providencia* were significantly elevated ($p < 0.05$) in infected frogs. Additionally, functional prediction confirmed that most of the microbiota in infected frogs were linked to metabolism-related KEGG pathways. In this study, the screened genes linked to immunity showed an association with the gut microbiome. The majority of these genes were found to be linked with the abundance of opportunistic pathogens. The results showed that *E. miricola* infection led to the downregulation of immune and metabolic-related genes, which led to the inhibition of immune function and metabolic disorder, and then increased the abundance of opportunistic pathogens in the gut microbiota. The findings of this study offer a preliminary foundation for comprehending the pathogenic processes of *E. miricola* infection in black spotted frogs.

Keywords: black spotted frog; *Elizabethkingia miricola*; transcriptome; gut microbiome

Key Contribution: The present study is important for discovering the pathogenic mechanism of *E. miricola* infection in black spotted frogs.



Citation: Wei, Q.; Wang, D.; Wei, K.; Xu, B.; Xu, J. The Mechanism of *Elizabethkingia miricola* Infection of the Black Spotted Frog as Revealed by Multi-Omics Analysis. *Fishes* **2024**, *9*, 91. <https://doi.org/10.3390/fishes9030091>

Academic Editor: Rex Dunham

Received: 28 December 2023

Revised: 20 February 2024

Accepted: 26 February 2024

Published: 28 February 2024



Copyright: © 2024 by the authors. Licensee MDPI, Basel, Switzerland. This article is an open access article distributed under the terms and conditions of the Creative Commons Attribution (CC BY) license (<https://creativecommons.org/licenses/by/4.0/>).

1. Introduction

The black spotted frog (*Pelophylax nigromaculatus*) (Hallowell, 1860) is predominantly distributed across East Asia. This amphibian species holds significant economic value in China owing to its tender musculature and abundant nutritional content. The breeding of

the black spotted frog is favored by farmers due to its low investment requirements, high output potential, and short breeding cycle [1]. Nevertheless, an intensive culture mode often brings serious diseases and leads to huge economic losses. Therefore, there is an urgent need to conduct research on these diseases and implement effective prevention and control measures to ensure the healthy and sustainable development of the black-spotted frog culture industry.

Elizabethkingia miricola, a Gram-negative bacterium that poses a threat to the lives of both humans and animals as it can cause disease [2,3], has been identified as the pathogen responsible for causing crooked head disease in black spotted frogs since 2016 [4]. Several studies have reported instances of varying anuran species displaying symptoms of crooked head disease, such as *Hymenochirus curtipes* [5], *Rana catesbeiana* [6], *Lithobates pipiens* [7], *Chinese spiny frog* [8], etc. This pathogen has emerged as a significant factor affecting the overall health of frogs.

E. miricola is widely distributed in the natural environment [9]. The challenge, however, comes with the treatment of the infection due to *E. miricola*'s preference for the brain as the predominant infection site, and the limited ability of existing pharmacological agents to penetrate the blood–brain barrier. Furthermore, the pathogenic mechanism of *E. miricola* is currently unclear, and the impact of its infection on the metabolism and immune function, as well as the intestinal microecology of the black spotted frog remains unknown.

Vertebrate gastrointestinal tracts house a rich diversity of microorganisms that have intricately evolved alongside their hosts and serve pivotal functions in regard to nutrition, metabolism, development, and immunity [10]. Several studies have demonstrated a correlation between the occurrence of bacterial and viral diseases and the composition of gut bacteria in animals [11].

Studies have shown that the intestinal microbiota is closely related to the upward and downward regulation of immune and metabolic pathways [12], and the analysis of intestinal microbiota and transcriptome data could help us clarify the pathogenesis of various diseases, and dissect the pathological mechanism of diseases to find therapeutic target [13].

In this study, we conducted an experiment involving artificial infection of black spotted frogs with *E. miricola*. We meticulously documented the observed clinical signs and proceeded to analyze and identify the transcriptomes of the liver and kidney, as well as the intestinal microbiome. Transcriptomics, a widely employed approach in animal studies, was utilized to gain a comprehensive understanding of the interactions between the host and the pathogen [14]. Comparative analyses of the transcriptomes in the livers and kidneys of both infected and uninfected with *E. miricola* were performed to elucidate the molecular evidence underlying the host's response to *E. miricola* infection. Additionally, we utilized a microbiome-based strategy to investigate the structure of the microbial community, offering significant knowledge of the pathogen's infection and transmission pathway [11,15]. Ultimately, the integration of transcriptomic and microbiomic analyses enabled us to uncover the mechanisms that trigger disease onset, by establishing connections between dysbiosis and host-related gene expression disparity [11].

2. Materials and Methods

2.1. Ethics Statement

The frogs used throughout the experiments were black spotted frogs. All animal experiments were conducted in accordance with the guidelines and approval of the Animal Experimental Ethical Inspection of Laboratory Animal Centre, Yangtze River Fisheries Research Institute, Chinese Academy of Fishery Sciences.

2.2. *Elizabethkingia miricola* Challenge Experiment and Frog Sampling

The *E. miricola* strain utilized in this experiment was acquired from the laboratory strain collection. The black spotted frogs (32.04 ± 7.59 g) were procured from a frog culture farm in Jingzhou City, Hubei province. Subsequently, they were acclimated within the

confines of the Ecological Aquaculture Group's laboratory at the esteemed Yangtze River Fisheries Research Institute of the Chinese Academy of Fishery Sciences for a duration of 5 days. The tanks employed possessed dimensions of $50 \times 33 \times 31$ cm, and were meticulously filled with well-aerated water, ensuring the frogs' thoraxes were positioned just below the water's surface. Throughout the domestication and experimental period, the frogs were not provided any sustenance. It is of utmost importance to note that all black spotted frogs remained in a state of optimal health and unscathed during the domestication process.

E. miricola, in the form of a 1×10^8 CFU/mL (LC50) suspension in sterile PBS, was meticulously prepared for subsequent infection experiments [16]. The total cohort of 40 domesticated black spotted frogs was evenly divided into experimental and control groups. The experimental group received an injection of 0.2 mL of a 1×10^8 CFU/mL suspension of *E. miricola*, while the control group received an injection of 0.2 mL of sterile PBS [1,16]. The probability of survival within 7 days was counted (Table S1). After a span of 24/48 h following the injection, the black spotted frogs were humanely euthanized through the medullary destruction method [17]. The frogs were promptly dissected upon cessation of their struggles, with their livers and kidneys carefully separated into RNA-enzyme-free tubes. The aforementioned organs were isolated into RNA-free tubes, supplemented with an ample quantity of RNA-kill reagent (Biosharp, Beijing, China), and expeditiously stored at -80°C for future utilization. Intestinal tissues were also segregated into RNA-free tubes and temporarily preserved at -80°C .

2.3. RNA Extraction, Library Construction, and Sequencing

According to the manufacturer's protocol, we used the Trizol reagent kit (Invitrogen, Carlsbad, CA, USA) to extract the total RNA, and a photometer was used to determine RNA sample integrity (Thermo Scientific, Waltham, MA, USA). After extracting the total RNA, the Ribo-Zero™ Magnetic Kit (Epicentre, Madison, WI, USA) was used to remove rRNA. Then, the enriched mRNA fragments were reverse transcribed into cDNA. The QiaQuick PCR extraction kit (Qiagen, Venlo, The Netherlands) was used to purify the cDNA fragments. The size of the connecting product was selected via agarose gel electrophoresis and PCR amplification, and sequencing was performed using Illumina Novaseq 6000 of Gene Denovo Biotechnology Co. (Guangzhou, China).

2.4. Analysis of Intestinal Microbiota

Twelve hindgut tissues (including the content) were collected. DNA was extracted using the HiPure Soil DNA Kit (Magen, Guangzhou, China) according to the protocol. Each group had three replicates. The V3–V4 hypervariable regions of the bacterial 16S rRNA gene were amplified with 341F(5'-CCTACGGGNGGCWGCAG-3') and 806R(5'-GGACTACHVGGGTATCTAAT-3') primers [18]. The PCR reactions were conducted using the following program: 3 min of denaturation at 94°C , 30 cycles of 40 s at 94°C , 30 s of annealing at 56°C , 60 s of elongation at 72°C , and a final extension at 72°C for 10 min. Purified amplicons were sent to Gene Denovo Biotechnology Co. (Guangzhou, China) for sequencing. The raw data underwent quality filtering using QIIME Pipeline-Version 1.9 [19], and then were merged via FLASH (version 1.2.11) with a minimum overlap of 10 bp and mismatch error rates of 2%. The chimerism was detected and low-quality sequences were removed using the Usearch software package V11 [20]. Operational taxonomic units (OTU) were clustered with $>97\%$ similarities. The UCLUST was used to locate these OTU in the Greengenes database (release 13.8) [20,21].

Krona (version 2.6) was used to visualize the statistics [22]. Alpha and beta diversity were calculated. Linear discriminant analysis coupled with effect size (Lefse) was used to study the significance of species' differences at the genus level [23]. The KEGG pathway analysis of the OTU was inferred using PICRUSt (version 2.1.4) [24].

2.5. Quantitative Real-Time PCR

To verify the transcriptome data, 11 randomly selected DEGs were examined via relative quantitative real-time PCR (RT-qPCR). The amplification steps were as follows: 95 °C for 2 min, 40 cycles of 95 °C for 30 s, 60 °C for 10 s, and 30 s at 75 °C. These DEGs used for verification included transaldolase 1 (*Taldo1*), lysosomal protein transmembrane 4 alpha (*LAPTM4A*), CD63 molecule (*CD63*), cathelicidin 2 (*CATHL2*), ribosomal 60S subunit protein L4B (*rpl4-b*), betaine-homocysteine S-methyltransferase (*bhmt*), Rac family small GTPase 2 (*RAC2*), myosin light chain 9 (*MYL9*), hemoglobin subunit alpha 2 (*hba2*), chymotrypsinogen B1 (*CTRB1*), and ATP synthase membrane subunit e (*Atp5me*) (Table 1). Normalized cDNA amounts were found using housekeeping gene β -actin. Three replicates were performed for each sample, and relative levels of gene expression were calculated using the $2^{-\Delta\Delta C_t}$ method.

Table 1. The primers used for validation of DEGs via RT-qPCR.

Primers for RT-qPCR	Primer Sequence (5' to 3')
<i>Actb</i> -F	CGTCCAGAGGCATACAGAGA
<i>Actb</i> -R	ACCCCAAAGCAAACCGAGAA
<i>Taldo1</i> -F	AAGCCACAGGATGCCACTAC
<i>Taldo1</i> -R	TAGAAACCCGACCAGGAACC
<i>LAPTM4A</i> -F	GAGGTTAGGAGGATTTCGCTG
<i>LAPTM4A</i> -R	GCCTGCGTGCTCTTTGC
<i>CD63</i> -F	AACACTTCACAGCCAGCCAG
<i>CD63</i> -R	CAAGCAGCAAGCAAAGACGA
<i>CATHL2</i> -F	TGTGACTACAAGGAGGACGG
<i>CATHL2</i> -R	GATTATTTCTGGTGAAGCGGAG
<i>rpl4-b</i> -F	CATCTGGACGGAGAGTGCC
<i>rpl4-b</i> -R	TGCCTTGGGTTTCTTTGCCT
<i>Bhmt</i> -F	CCCAACAACAGAGGCACCA
<i>Bhmt</i> -R	ATGTGGAAGAGGCAGTGTGG
<i>RAC2</i> -F	GAAAGGGTCGGTGGCAAAGG
<i>RAC2</i> -R	ACCAAAAGCCCCAAGTGTGT
<i>MYL9</i> -F	GAATGGTGCTGCCGAGGTAA
<i>MYL9</i> -R	GGAGCCAAAGACAAGGATGA
<i>hba2</i> -F	GTTTCGCCGTCCAGTTTGT
<i>hba2</i> -R	TGCCCTATTTACCTCTTGCT
<i>CTRB1</i> -F	TCCAGAATCGTGAATGGTGAGG
<i>CTRB1</i> -R	GTGGTTGAGCAGTGACAGGAG
<i>Atp5me</i> -F	AAGTGTCCCCGCTCATCAA
<i>Atp5me</i> -R	CCTCTGCCTCAATCCTTCTGT

3. Results

3.1. Analysis of Differentially Expressed Genes

By comparing the liver transcriptome profiles of black spotted frogs in control and infected groups, we identified a total of 1469 DEGs, of which 544 genes were upregulated and 925 genes were downregulated (Figure 1). In the kidney, a total of 4737 DEGs were identified, of which 2164 genes were upregulated and 2573 genes were downregulated (Figure 2).

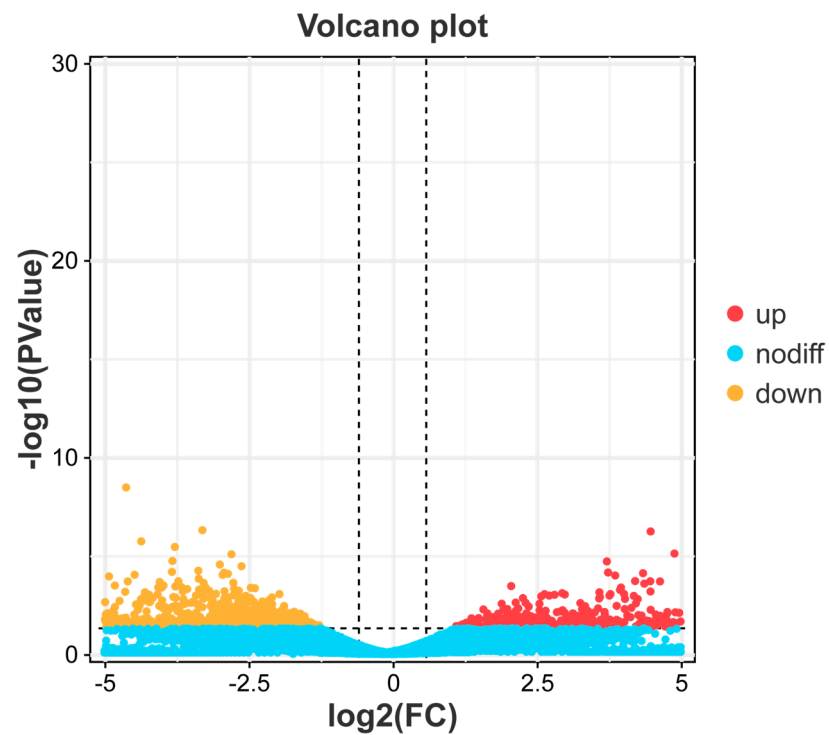


Figure 1. “Volcano plot” of DEGs in liver. The red dots represent genes that are significantly upregulated. The yellow dots represent genes that are significantly downregulated. The blue dots represent genes that are no significant differences.

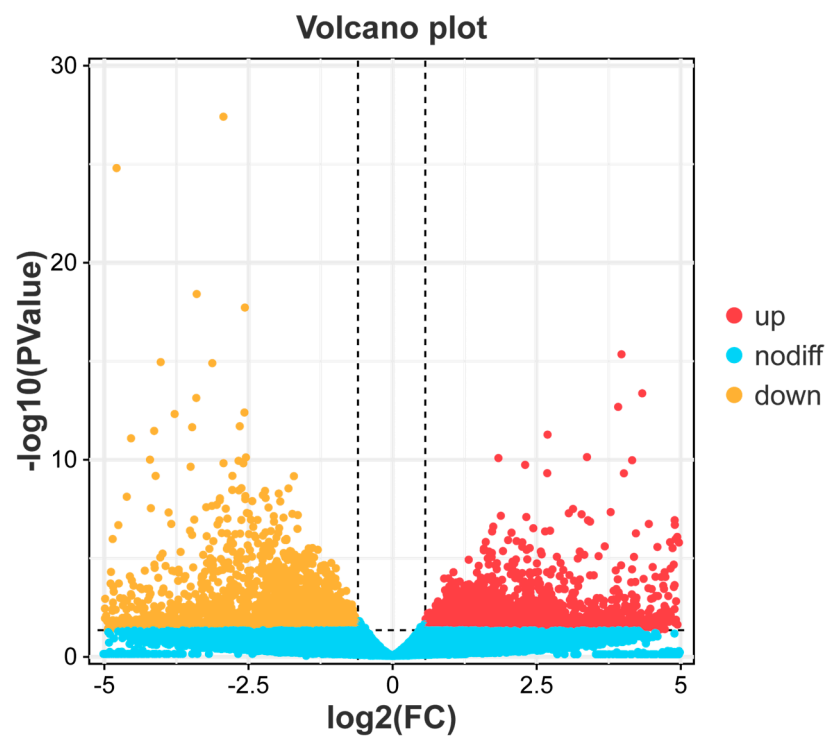


Figure 2. “Volcano plot” of DEGs in kidney. The red dots represent genes that are significantly upregulated. The yellow dots represent genes that are significantly downregulated. The blue dots represent genes that are no significant differences.

3.2. Liver Transcriptome Function Analysis

The GO functional annotation of the 1469 DEGs identified from the LE-48 liver samples unveiled a notable downregulation in crucial biological processes such as “Cellular process”, “Metabolic processes”, and “response to stimulus”. Similarly, in terms of molecular functions, a significant decrease was observed in the categories of “binding” and “catalytic activity” for the majority of the DEGs (Supplementary Figure S2).

Further examination of the GO term enrichment through the Go enrichment bar chart highlighted the prominence of organismal immunity-related processes. Notably, the top five enriched GO terms were all associated with immune responses, including immune response, immune effector processes, leukocyte-mediated immunity, immune system processes, and myeloid-leukocyte-mediated immunity. Remarkably, among the top 30 enriched GO terms, 10 were directly related to immune function (Figure 3). This comprehensive analysis strongly indicates a severe impairment of the immune system in black spotted frogs infected with *E. miricola*, ultimately leading to disease progression and mortality.

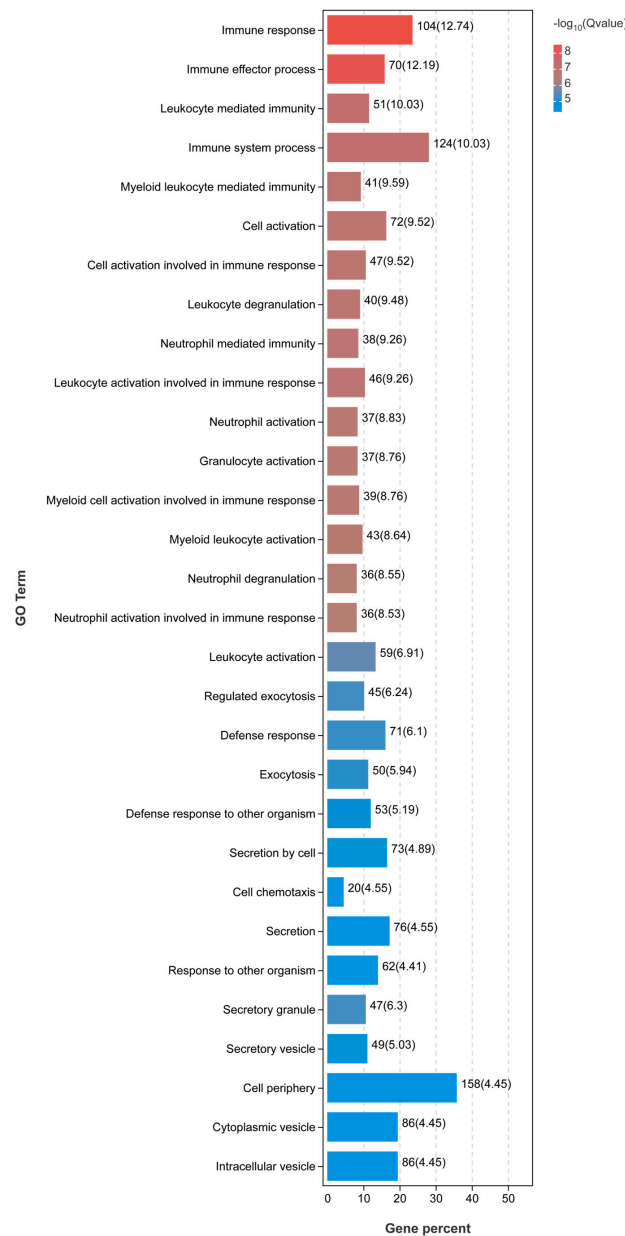


Figure 3. GO enrichment analysis of DEGs in liver.

The KEGG analysis was conducted to gain deeper insights into the altered transcriptional functions in *E. miricola*-infected black spotted frogs. The outcomes revealed that the liver of LE-48 exhibited enrichment in diverse pathways, prominently encompassing immune response, metabolic pathways, and bacterial infection. Notably, the immune response pathways comprised neutrophil extracellular trap formation, the NOD-like receptor signaling pathway, leukocyte transendothelial migration, chemokine signaling pathway, and Fc Gamma R-mediated phagocytosis. Remarkably, a majority of these immune-related signaling pathways exhibited significant upregulation. Additionally, metabolic pathways such as the pentose phosphate pathway, carbon metabolism, glycerophospholipid metabolism, and glycerolipid metabolism were observed (Figure 4). Furthermore, pathways associated with disease infection, including *Staphylococcus aureus* infection, Leishmaniasis, Legionellosis, and Shigellosis were identified.

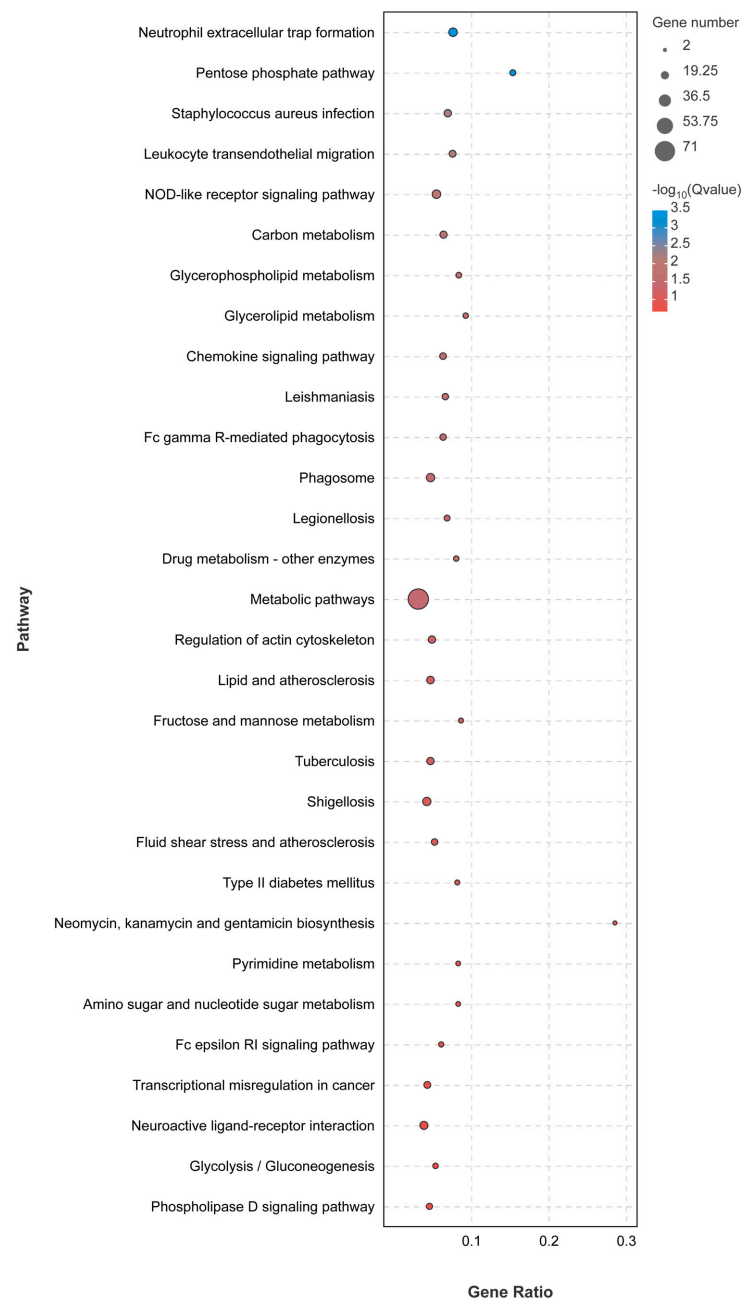


Figure 4. KEGG pathway analysis of DEGs in liver.

In this investigation, our objective encompassed the characterization of immune-related genes that undergo activation in response to the infection caused by *E. miricola*. Through meticulous screening, we successfully identified a repertoire of crucial genes intricately associated with the mechanisms of immunity and defense in the black spotted frogs subjected to *E. miricola* infection. Notably, the following ten genes were identified: *Nlrp3*, *NAIP*, *GBP4*, *CLEC4M*, *C3*, *CYBB*, *CXCR1*, *CASP3*, *Mr1*, and *MMP3* (Table 2).

Table 2. Differentially significant immune-related genes in the liver during black spotted frog response against *E. miricola*.

Gene ID	Annotation	Log2fc	p-Value
<i>CASP3</i>	caspase 3	12.95595	4.16×10^{-9}
<i>Mr1</i>	major histocompatibility complex, class I-related	4.073231	0.011
<i>MMP3</i>	matrix metalloproteinase 3	3.588169	0.000742
<i>CXCR1</i>	C-X-C motif chemokine receptor 1	-2.96424	0.018407
<i>CYBB</i>	cytochrome b-245 beta chain	-3.30264	0.000655
<i>C3</i>	complement C3	-3.71698	0.000203
<i>CLEC4M</i>	C-type lectin domain family 4 member M	-4.19152	0.021062
<i>NAIP</i>	NLR family apoptosis inhibitory protein	-4.41834871	0.005662
<i>GBP4</i>	guanylate binding protein 4	-9.52290841	0.03983
<i>Nlrp3</i>	NLR family pyrin domain containing 3	-10.5209	0.014988

3.3. Kidney Transcriptome Function Analysis

GO functional annotation of 4737 DEGs screened from KE-48 kidneys revealed a significant downregulation in biological processes related to “Cellular processes”, “Metabolic processes”, and “Biological regulation”. Similarly, in the molecular function classification, a significant downregulation was observed in terms of “binding” and “catalytic activity” for the majority of DEGs (Supplementary Figure S3).

Further analysis of the enrichment of each GO term using the Go enrichment bar chart highlighted the top five enriched functions associated with organismal immunity, including “immune response”, “immune system processes”, “Leukocyte-mediated immunity”, “inflammatory response”, and “immune effector processes”. Remarkably, among the top 30 enriched GO terms, 14 were directly related to immune functions (Figure 5). These findings strongly indicate a severe impairment of the immune system in black spotted frogs infected with *E. miricola*, ultimately leading to disease progression and mortality.

The DEGs were subjected to KEGG analysis to gain deeper insights into the transcriptional changes occurring in infected black spotted frogs. The outcomes revealed that the kidney of KE-48 exhibited enriched pathways primarily associated with immune response and bacterial infection. Notably, the immune-related pathways encompassed neutrophil extracellular trap formation, the NOD-like receptor signaling pathway, B cell receptor signaling pathway, C-type lectin receptor signaling pathway, complement and coagulation cascade, NF- κ B signaling pathway, as well as Toll-like receptor signaling pathway. Additionally, pathways linked to “disease infections”, including *Staphylococcus aureus* infection, Tuberculosis, Pathogenic *Escherichia coli* infection, *Legionellosis*, and *Yersinia* infection were predominantly downregulated (Figure 6).

Likewise, we conducted a comprehensive analysis and discernment of pertinent immune genes, culminating in the identification of pivotal genes intricately linked to the realm of immunity and the fortification of defense mechanisms post-infection. Notably, these genes encompass *Cfl*, *HLA-DRA*, *IGHV2-26*, *MPO*, *NLRP12*, *Prkcd*, *Cxcl9*, *Mr1*, *CASP3*, and *MMP3* (Table 3).

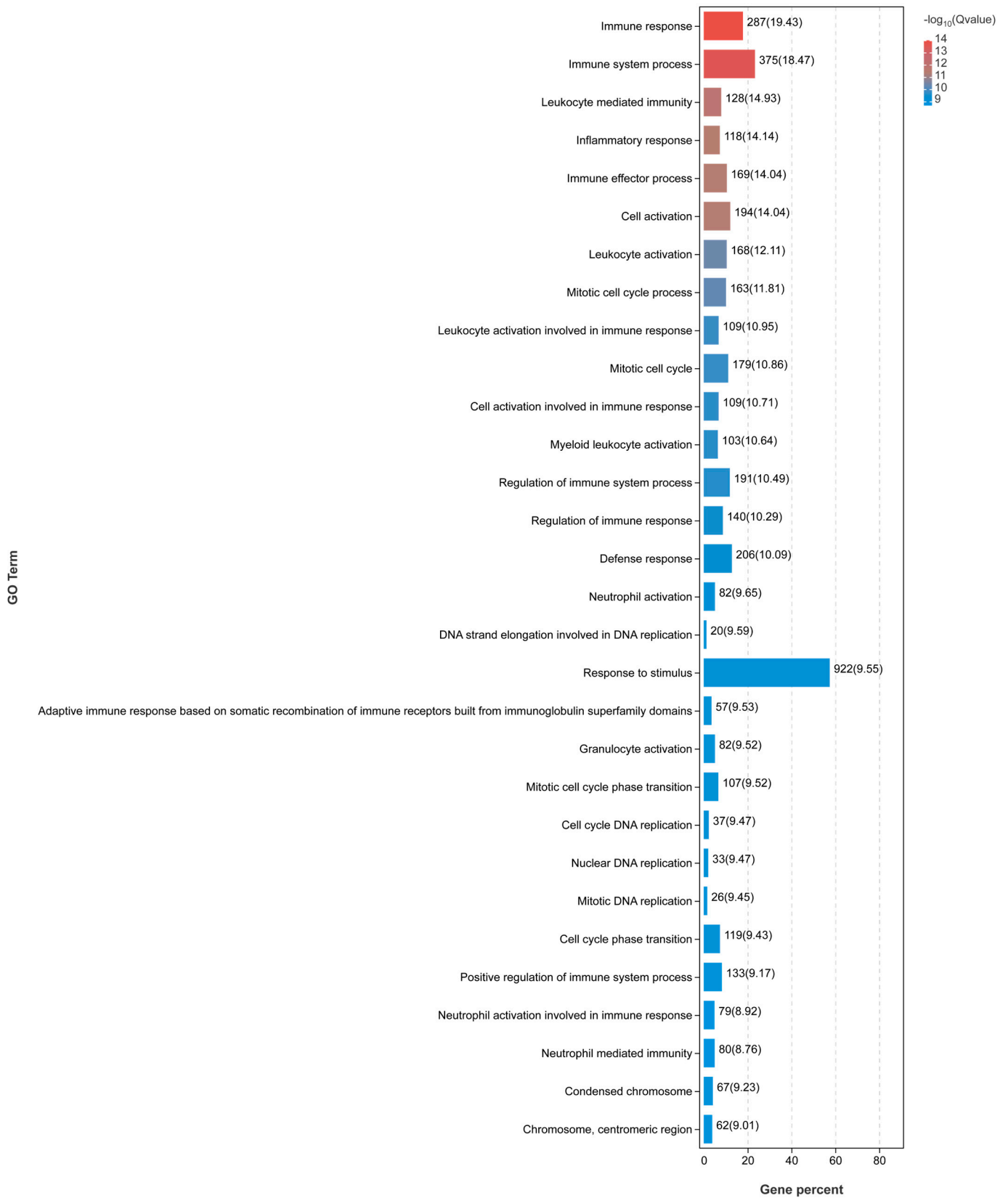


Figure 5. GO enrichment analysis of DEGs in kidney.

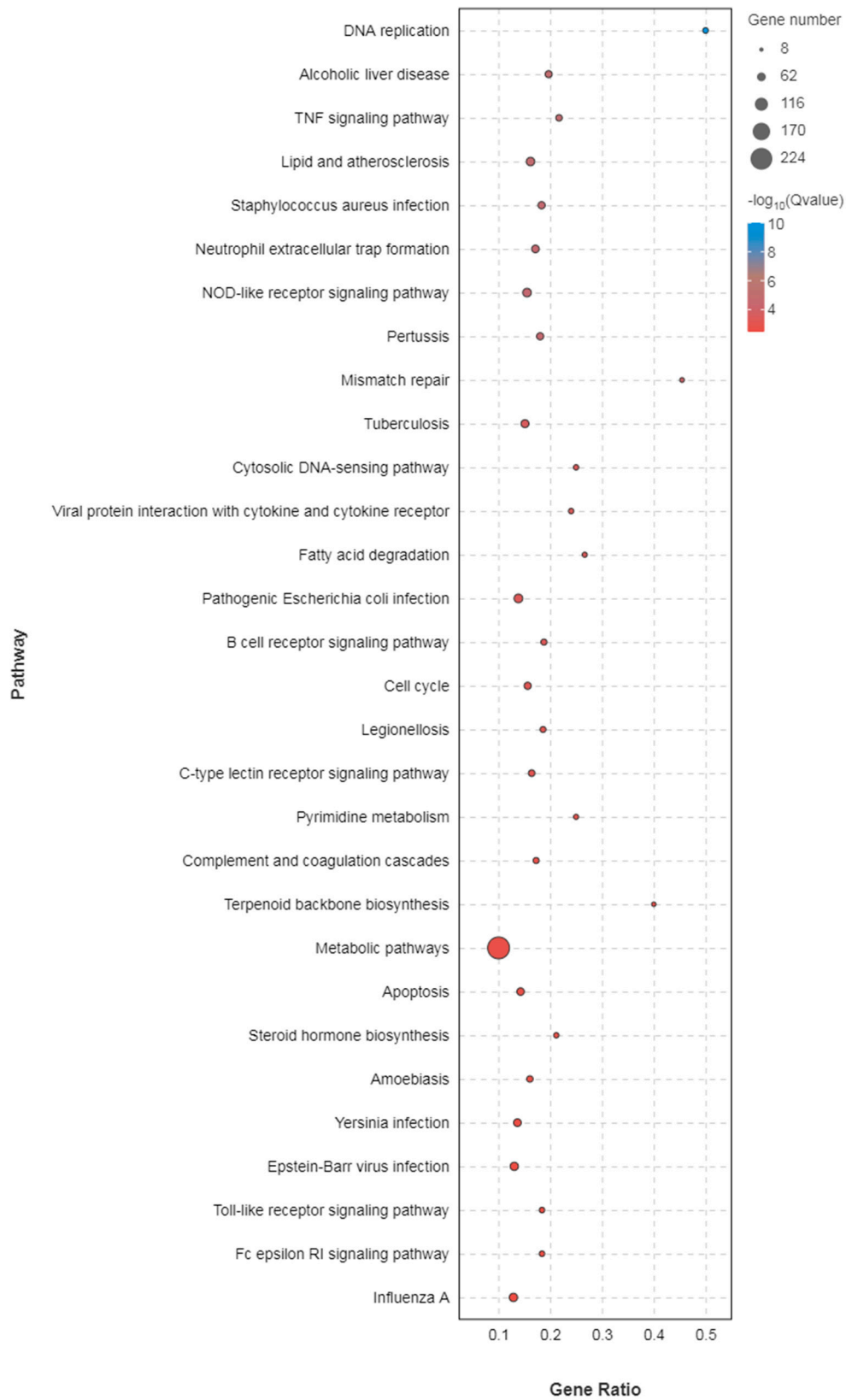


Figure 6. KEGG pathway enrichment analysis of DEGs in kidney.

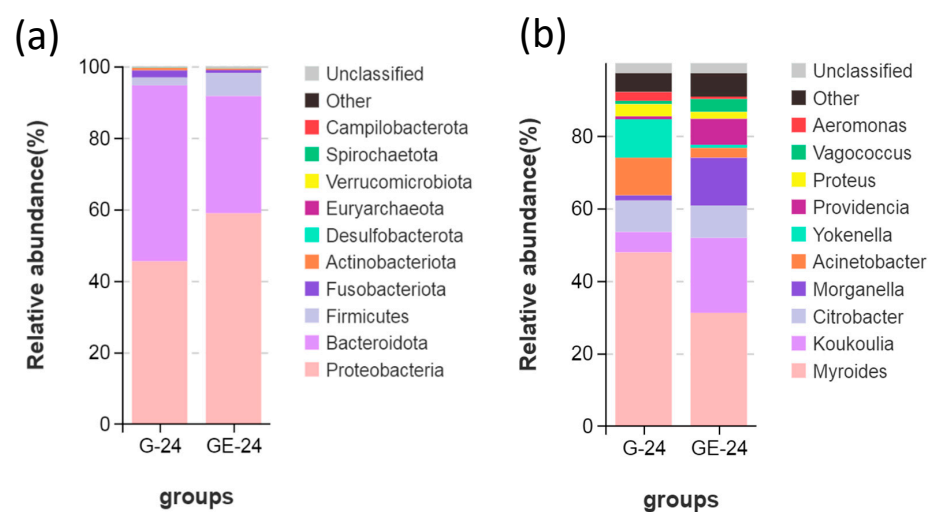
Table 3. Differentially significant immune-related genes in the kidney during black spotted frog response against *E. miricola*.

Gene ID	Annotation	Log2fc	p-Value
<i>NLRP12</i>	NLR family pyrin domain containing 12	10.37032	0.037796
<i>Mr1</i>	major histocompatibility complexes, class I-related	8.930455	0.000588
<i>CASP3</i>	caspase 3	6.589579	1.05×10^{-24}
<i>Prkcd</i>	protein kinase C delta	3.943372	0.038313
<i>Cxcl9</i>	C-X-C motif chemokine ligand 9	1.894896	7.80×10^{-8}
<i>MMP3</i>	matrix metalloproteinase 3	1.879163	0.003148
<i>MPO</i>	Myeloperoxidase	−3.4607	2.49×10^{-12}
<i>IGHV2-26</i>	immunoglobulin heavy variable 2-26	−6.63979	0.013474
<i>HLA-DRA</i>	major histocompatibility complex, class II, DR alpha	−10.2669	1.83×10^{-74}
<i>Cfh</i>	complement factor H	−14.7934	0.009374

3.4. Analysis of Intestinal Microbiota

A total of 885 OTU were acquired, 203 (22.9%) OTU were found to be shared between groups, 262 (29.6%) were exclusively present in the healthy group, and 420 OTU (47.4%) were exclusively found in the infected group (Figure S4). Notably, no significant disparities in alpha diversity (Simpson, ACE, Chao1, Shannon) were observed between the groups (Simpson: $p = 0.4$; ACE: $p = 0.7$; Chao1: $p = 0.7$; Shannon: $p = 0.7$) (Supplementary Figure S5). Also, there was no significant difference in the Bray–Curtis and Jaccard algorithms (Bray–Curtis: $p = 0.3$; Jaccard: $p = 0.2$) (Supplementary Figure S6). However, principal coordinate analysis (PCoA) revealed the potential to discriminate between the bacterial communities of the two groups (Supplementary Figure S7).

At the phylum level, Proteobacteria, Bacteroidota, Firmicutes, and Fusobacteriota emerged as the prevailing taxa within the intestinal microcosm of both uninfected and infected black spotted frogs. Remarkably, the infected group exhibited a notably augmented relative abundance of two distinguished phyla, namely Proteobacteria and Firmicutes, in comparison to the uninfected group (58.87% vs. 45.45% and 6.50% vs. 2.16%, respectively). Conversely, the relative abundance of Bacteroidota and Fusobacteriota was significantly diminished in the infected group compared to the uninfected group (32.79% vs. 49.24% and 0.79% vs. 1.99%, respectively) (Figure 7a).

**Figure 7.** Microbial composition in the gut of black spotted frogs, (a,b) represent the dominant phyla and genera in groups.

At the genus level, the infected frogs exhibited a substantial escalation in the relative abundance of four genera, namely *Koukoulia* (20.68% vs. 5.64%), *Morganella* (13.18% vs. 1.39%), *Providencia* (7.23% vs. 0.84%), and *Citrobacter* (8.89% vs. 8.5%) (Figure 7b).

Based on Lefse analysis, a comprehensive examination of 11 taxa revealed notable variations in abundance between infected and uninfected frogs. Notably, certain opportunistic pathogens, such as *Morganella* and *Shewanella*, exhibited substantially higher Linear Discriminant Analysis (LDA) scores in infected frogs, indicating their potential significance in pathogenicity and mortality within the frog population (Figure 8).

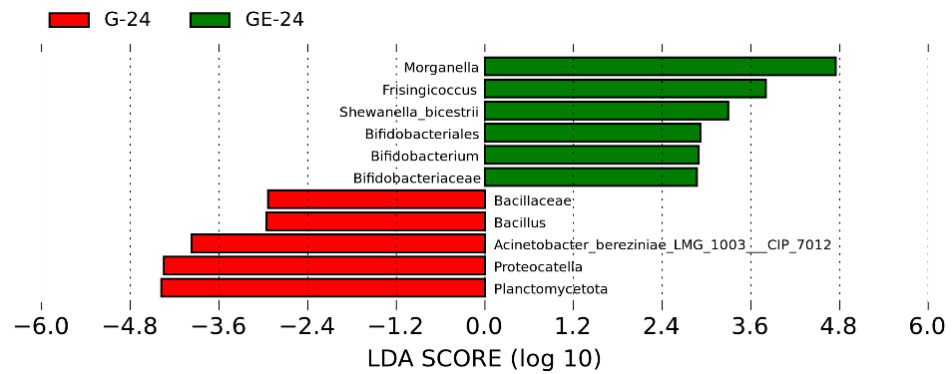


Figure 8. Bacterial taxa with significant differences (LDA score > 2.0) in the relative abundance identified by Lefse in uninfected and infected groups (G24 vs. GE24).

However, in the lefse analysis conducted at the 48 h time point post-infection, the differential changes in abundance between the two groups were more pronounced compared to the 24 h time point. Interestingly, we observed that certain conditionally pathogenic bacteria, such as *Morganella* and *Shewanella*, which initially exhibited higher abundance in the infected group, were no longer significantly different (Figure 9). This suggests that the immune system may have played a crucial role in restoring the organism’s homeostatic balance by the 48 h mark following infection with *E. miricola*. Remarkably, our findings revealed no further mortality among the black spotted frogs at the 48 h time point post-infection.

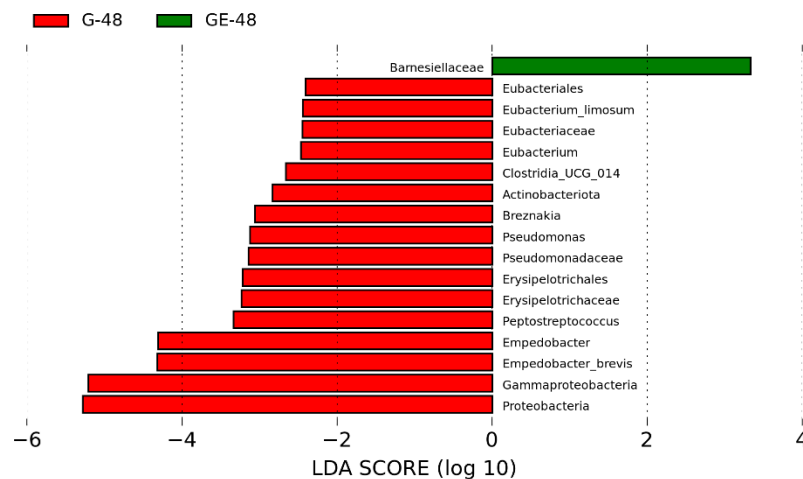


Figure 9. Bacterial taxa with significant differences (LDA score > 2.0) in the relative abundance identified by Lefse in uninfected and infected groups (G-48 vs. GE-48).

Moreover, the functional prediction of OTU using PICRUST2 revealed a predominant association of the gut microbiota in infected black spotted frogs with pathways primarily related to metabolism (Figure 10). This observation implies that infection by *E. miricola* could potentially disrupt the metabolic processes within the organism.

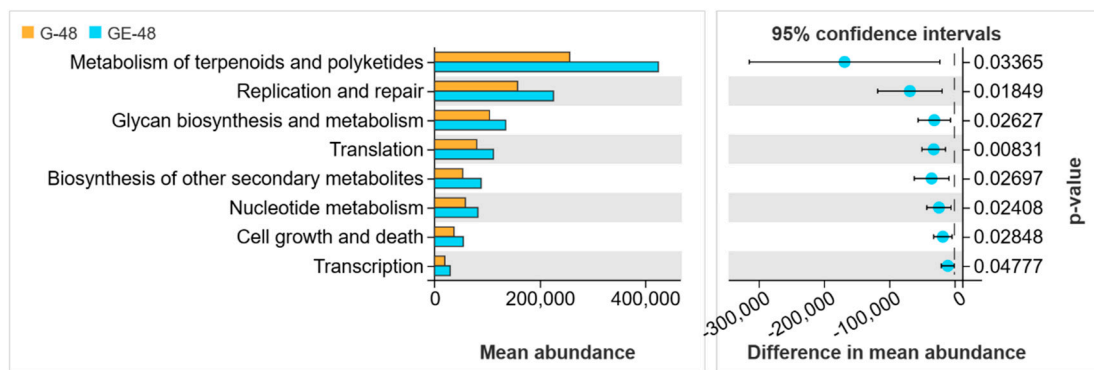


Figure 10. Function prediction of gut bacteria in black spotted frogs. G-48 and GE-48 represent the uninfected and infected groups, respectively.

3.5. Intestinal Microbiota and DEG Association Analysis

In the context of liver and kidney tissues, a comprehensive investigation was conducted to explore the intricate relationship between the abundance of intestinal microbiota and the expression of immune-related genes. To establish this connection, Spearman correlation analysis was employed, enabling the construction of a correlation network diagram.

In the liver, our findings revealed a positive correlation between the abundance of *E. miricola* in the gut and the expression of the *Mr1* and *C3* genes. This observation suggests that these two immune genes may hold pivotal roles in the context of infection. Additionally, it was observed that *mr1* exhibited correlations with the abundance of various opportunistic pathogens, including *Edwardsiella*, *Shigella*, and *Providencia*. Conversely, the abundance of probiotic bacteria in the gut demonstrated a significant association with *GBP4*, *NAIP*, *CXCR1*, *CYBB*, and *CLEC4M*. Notably, the strongest correlation was observed between *Bacillus* and the expression of *CXCR1*, *CYBB*, and *CLEC4M* (Figure 11). These findings imply that these five immune genes primarily contribute to the regulation of the intestinal microbiota, enabling the host to combat pathogenic infections effectively.

In the kidney, our findings mirrored those observed in the liver. The intestinal abundance of *E. miricola* exhibited positive correlations with the expression of *Mr1*, *Cfh*, and *MPO* genes, where *Cfh*, akin to *C3*, holds significance as a key component of the complement system. Furthermore, we noted that the expression of *Prkcd* and *HLA-DRA* genes correlated with the abundance of diverse commensal bacteria in the intestinal tract, indicating a crucial pathway for the organism's regulation of the gut microbiota (Figure 12). Additionally, the expression of other immune-related genes displayed associations primarily with the abundance of opportunistic pathogenic bacteria.

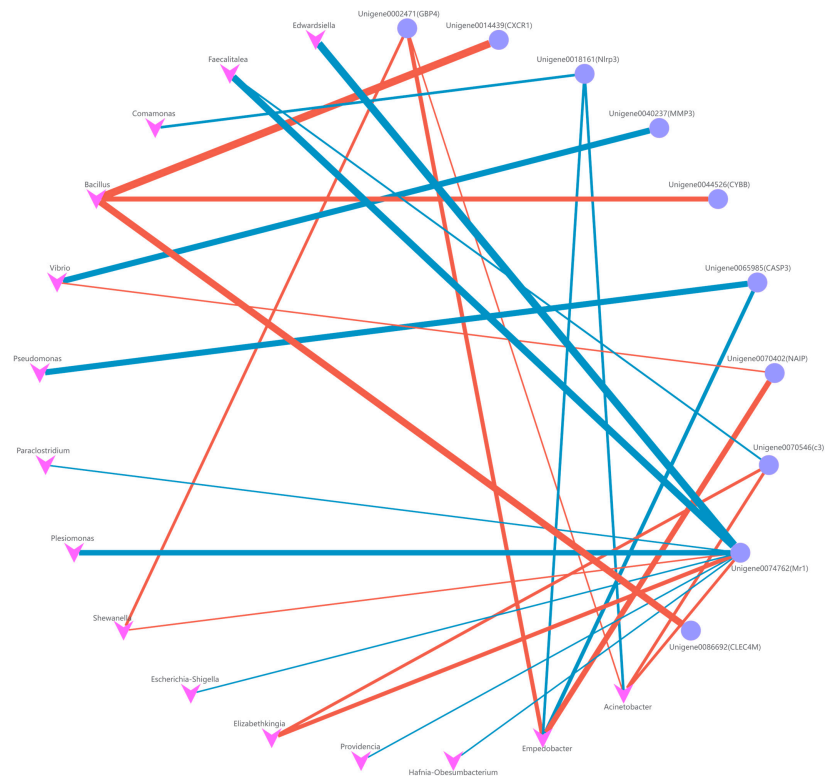


Figure 11. Co-occurrence network (FDR < 0.01) between the genus level (top 30) of intestinal microbiota and immune-related DEGs in liver. The blue line shows the negative correlation between genes and genera; the red line shows the positive correlation between genes and genera.

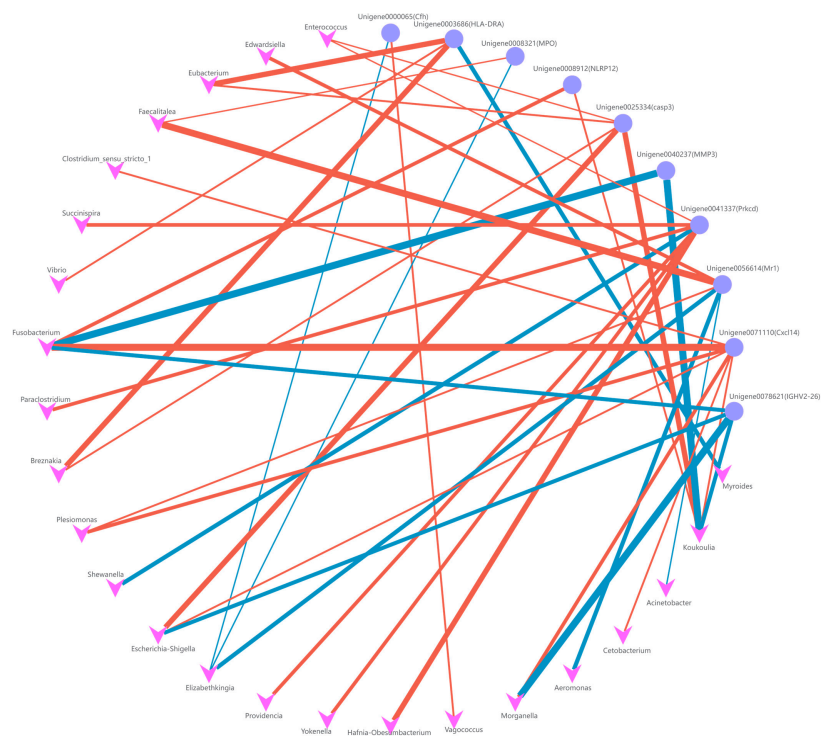


Figure 12. Co-occurrence network (FDR < 0.01) between the genus level (top 30) of intestinal microbiota and immune-related DEGs in kidney. The blue line shows the negative correlation between genes and genera; the red line shows the positive correlation between genes and genera.

4. Discussion

In this study, we conducted a comprehensive analysis of transcriptomic data obtained from the liver and kidney tissues of black spotted frogs following a 48 h infection with *E. miricola*. Through GO and KEGG enrichment analyses, we identified the most prominent pathways, namely immune response, metabolic response, and infectious disease (bacterial), which exhibited significant differences pre- and post-infection.

The liver, renowned as a pivotal organ for metabolism, assumes a crucial role in nutrient absorption from the gut and subsequent transportation to its tissues. Recent scientific investigations have underscored the intricate interplay between the immune system and liver metabolism [25].

In this study, gene transcripts were comparatively analyzed in the livers of infected and uninfected black spotted frogs to unveil the main impact of *E. miricola* infection on the host immune system. Based on the transcriptome, a greater number of downregulated genes were observed in infected black spotted frogs, suggesting that *E. miricola* infection may impede certain physiological functions of the host. KEGG pathway enrichment analysis revealed that a majority of the differentially expressed genes (DEGs) were associated with body metabolism, including the pentose phosphate pathway, carbon metabolism, glycerophospholipid metabolism, and glycerolipid metabolism. Recent research has revealed that the pentose phosphate pathway not only influences the energy demands of pathogens, but also exerts a direct impact on their capacity to actively contribute to the pathogenesis of organisms. [26]. The glycerophospholipid metabolic pathway is also involved in a variety of diseases [27].

As a response to pathogen infection, the host will initiate a robust immune response against the pathogen. Seven out of ten immune-related DEGs including *Nlrp3*, *NAIP*, *GBP4*, *CLEC4M*, *C3*, *CYBB*, and *CXCR1* were significantly downregulated in infected black spotted frogs. Many infection and stress signals can rapidly activate *Nlrp3* inflammasome and *NAIP*, triggering a strong inflammatory response [28]. Previous studies have shown that the complement system is activated by the establishment of the cleavage membrane attack complex (MAC), which disrupts the cell membrane of invading pathogens to defend against bacterial infection [29]. These downregulated genes imply that *E. miricola* may suppress the host immune response, thereby facilitating its proliferation and subsequent development of conditionally pathogenic infections, ultimately resulting in host mortality. Notably, among the significantly upregulated genes, the expression of *Mr1* in infected frogs exhibited a $\log_2\text{fc}$ value of 4.073. It has been demonstrated that the overexpression of *Mr1* leads to the global dysregulation of numerous immune-related genes [30]. Matrix metalloproteinase 3 (*MMP3*), commonly referred to as stromelysin-1, exhibited a $\log_2\text{fc}$ value of 3.588 in our investigation. This multifaceted enzyme has been identified as a key player in a diverse array of cellular biological phenomena, demonstrating its integral involvement in numerous immune-mediated disorders and pathogen-induced pathologies [31]. *MMP3* is widely regarded as a ubiquitous inflammatory mediator that instigates inflammatory responses across various organ systems, including the intricate network of the nervous system [32]. We postulate that *MMP3* assumes a significant role in infection by *E. miricola*; however, the precise mechanism necessitates further elucidation.

Furthermore, it is worth mentioning that *HLA-H* and *H2-Aa* exhibited $\log_2\text{fc}$ values of 5.724 and 2.84, respectively. Notably, these genes, along with *Mr1*, are intricately linked to the synthesis of the major histocompatibility complex (MHC) class II protein complex. The MHC class II antigen presentation pathway serves as a pivotal connection between the innate and adaptive immune responses [33]. Therefore, we postulate that the MHC class II antigen presentation pathway may serve as the principal immune mechanism in the black spotted frog to combat *E. miricola* infection.

The KEGG pathway enrichment analysis conducted on kidney transcriptomics data revealed a notable suppression of immune-related pathways in infected black spotted frogs. Notably, pathways such as the NOD-like signaling pathway, TNF signaling pathway, B-cell signaling pathway, and C-type lectin receptor signaling pathway exhibited significant

downregulation. In this investigation, our focus was directed towards the NOD-like signaling pathway and TNF signaling pathway. The TNF pathway bears a close association with the intricate process of apoptosis. Within the apoptosis program, the pivotal role is assumed by the Caspase protein family, wherein *casp8* serves as the catalyst for apoptosis initiation, while *casp3* and *casp7* act as the executors of this intricate cellular mechanism [34]. Our investigation revealed remarkable distinctions in the \log_2fc values of *casp3*, *casp7*, and *casp8*, measuring 6.6, -8.8 , and -1.3 , respectively. These significant variations ultimately culminated in the occurrence of apoptosis, consequently leading to renal injury.

The NOD-like signaling pathway encompasses key genes, namely *Nlrp3*, *Nlrp12*, *Nlrp1*, and *Nlrp1a*. These genes exhibited substantial differential changes, as evidenced by their respective \log_2fc values of -2.6 , 10.4 , -2.69 , and -3.7 .

The NOD-like receptor protein, 1 (*Nlrp1*) inflammasome, plays an important role in the innate immune response. It promotes the activation of cysteinyl aspartate-specific protease (Caspase), which further activates interleukin 18 and interleukin 1β and mediates cellular pyroptosis [35], and is also important in traumatic central nervous system injury.

Recent investigations have unveiled the pivotal involvement of mixed lineage kinase domain-like (*MLKL*) proteins in orchestrating the assembly of extracellular meshworks, known as traps, in a manner contingent upon the *Nlrp3* inflammasome. Remarkably, the absence of *MLKL* instigates inflammasome activation impairment, leading to a compromised release of interleukin 18 (*IL-18*) and interleukin 1β (*IL-1\beta*). Our own empirical findings parallel these discoveries, as we observed a noteworthy downregulation of *MLKL*, *Nlrp3*, *IL-18*, and *IL-1\beta*. Consequently, we postulate that *IL-1\beta* infection detrimentally hampers the host's immune defenses by impeding *MLKL* expression, thereby perturbing the *Nlrp3* inflammasome–extracellular trap axis and ultimately fostering susceptibility to infection [36].

According to recent research, *Nlrp12* has been implicated in the suppression of neuroretinal autoimmunity [37]. In addition, due to the loss of *Cfh*, the functional and structural protection of the retina will be impaired, which is manifested by impaired visual function [38]. Significant downregulation of *Nlrp12* and *Cfh* was also found in our study. Therefore, we speculate that the downregulation of *Nlrp12* and *Cfh* may be related to cataracts and visual impairment after infection in black spotted frogs.

Among the downregulated immune-related genes, the enzyme, myeloperoxidase (*MPO*), predominantly resides within neutrophils, where it orchestrates the release of reactive halogen species (RHS) during inflammatory processes, thereby assuming a bactericidal role [39], and the reason for the inhibition may be based on the self-protection mechanism of *E. miricola* against removal. Among the upregulated immune genes, a partial convergence with the liver transcriptome was observed, delineating distinctive variances primarily within the *Nlrp12* and *CXCL9* genes. *CXCL9*, a formidable and efficacious biomarker, has been established for the evaluation of acute kidney injury. Remarkably, our study also detected an upregulated expression of *CXCL9*, presumably attributable to renal damage inflicted directly or indirectly by *E. miricola* infection [40]. Meanwhile, a study reported that *Salmonella enterica* and *Chlamydia trachomatis* inhibited *CXCL10* expression and suggested that *CXCL10* inhibition is an aggregation mechanism for immune evasion [41]. This is consistent with our results, where we also found significant downregulation of *CXCL10* in our study. Furthermore, intriguingly, within the KEGG-enriched pathway, we discerned a multitude of pathogen-associated infections such as *Staphylococcus aureus* infections, *Legionella* infections, *Shigella*-like infections, and *Yersinia* infections. We postulate that the fatality of *E. miricola* infection in the black spotted frog may stem from its suppression and devastation of the immune system, thereby instigating the onset of other opportunistic pathogenic infections in the surroundings subsequent to the coagulation or even annihilation of the frog's immune functionality, ultimately culminating in demise.

Imbalances in microbial communities in susceptible hosts may lead to opportunistic pathogen invasion and immune-mediated disease [42].

However, in the present study, no significant alterations were observed in the alpha diversity of the gut microbiota of the black spotted frog following infection. This implies that the impact of *E. miricola* infection might be limited to a fraction of the gut microbial community.

Among the identified phyla in the frog's intestine, Proteobacteria, Bacteroidota, Firmicutes, and Fusobacteriota were found to be the prevailing groups. Remarkably, the relative abundance of three opportunistic pathogens, namely *Morganella* (13.18% vs. 1.39%), *Providencia* (7.23% vs. 0.84%), and *Citrobacter* (8.89% vs. 8.5%), exhibited a significant increase in infected black spotted frogs.

Morganella is an important human conditional pathogen and has a potential role in aquatic pathogens. Recent studies have shown that it is capable of naturally infecting farmed bullfrogs and causing significant mortality [43]. It is hypothesized that the lethality in black spotted frogs infected with *E. miricola* may be related to *Morganella* as well. *Providencia* species are a rare group of opportunistic pathogens. They have been found to cause pathogenesis in *Labeo rohita* [44]. In alligators, *Providencia* infections have resulted in high mortality among *Mississippi alligators* reared under intensive farming conditions. Clinical manifestations included lethargy, poor body condition, and neurological signs such as head tilt and spinning. Histopathological analysis revealed pneumonia, hepatitis, and splenitis accompanied by heterophilic meningoencephalitis [45]. These symptoms bear some resemblance to those observed in *E. miricola* infections, where infected black spotted frogs also exhibited sluggish movement, head tilting, and inflammatory responses in various tissues.

Some *Citrobacter*, such as *Citrobacter fumigatus*, are a common pathogen in aquaculture, and are also capable of causing severe infections in American bullfrogs [46].

As intestinal commensals and symbiotic organisms, it was hypothesized that the reduction in Bacteroidota prevalence may be associated with *E. miricola* infection in this study. Currently, there is conclusive evidence demonstrating that Bacteroidota, via their metabolites (e.g., podocarp polysaccharide A), can inhibit bacterial and viral infections whilst also modulating host immune response strategies [47,48].

Nevertheless, a decrease in the prevalence of Bacteroidota was observed subsequent to infection in this investigation, presumably attributed to the proliferation of various opportunistic pathogens within the gastrointestinal tract. This proliferation, in turn, led to nutrient insufficiencies, ultimately suppressing the capacity of Bacteroidota to sustain the overall equilibrium of the gut microbiota ecosystem. Nonetheless, additional validation is required to ascertain the resistance of Bacteroidota against infection in black spotted frogs.

5. Conclusions

E. miricola severely affects the immune-related functions of infected black spotted frogs, resulting in significant downregulation of immune-related genes in the liver and kidney, resulting in neurological and immune system damage. The increased abundance of some opportunistic pathogenic bacteria (*Morganella*, *Shewanella*, *Citrobacter*, etc.) is also associated with infection with *E. miricola*, which may be an important cause of pathogenicity and lethality in black spotted frogs after infection. The present study is important for discovering the pathogenic mechanism of *E. miricola* infection in black spotted frogs.

Supplementary Materials: The following supporting information can be downloaded at: <https://www.mdpi.com/article/10.3390/fishes9030091/s1>. Table S1. The probability of survival within 7 days; Table S2. Data of RNA-seq; Figure S1. Quantitative real-time RT-PCR for validation of RNA-seq; Figure S2. Gene ontology (GO) enrichment analysis of DEGs in liver; Figure S3. Gene ontology (GO) enrichment analysis of DEGs in kidney; Figure S4. Numbers and sequence proportions of Shared OTUs between uninfected and infected groups; Figure S5. Alpha diversity of microbial communities in the intestines of uninfected and infected black spotted frog; Figure S6. Beta diversity of microbial communities in the intestines of uninfected and infected black spotted frog; Figure S7. Principal coordinates analysis (PCoA) of bacterial community structures.

Author Contributions: Conceptualization, J.X.; methodology, Q.W.; software, Q.W.; validation, D.W.; formal analysis, B.X.; investigation, K.W.; resources, J.X.; data curation, Q.W.; writing—original draft preparation, Q.W.; writing—review and editing, J.X.; visualization, D.W.; supervision, J.X.; project administration, J.X.; funding acquisition, J.X. All authors have read and agreed to the published version of the manuscript.

Funding: This work was supported by the National Key Research and Development Project (2019YFD0900305, 2018YFD0901303).

Institutional Review Board Statement: In June 2022, the animal study was reviewed and approved by the Animal Experimental Ethical Inspection of Laboratory Animal Centre, Yangtze River Fisheries Research Institute, Chinese Academy of Fishery Sciences. The study was conducted in accordance with the local legislation and institutional requirements (Approval Code: YF12022XJ01).

Data Availability Statement: The raw RNA sequencing data have been deposited in the NCBI Sequence Read Archive under BioProject accession number PRJNA1055280.

Acknowledgments: We sincerely thank anonymous reviewers for their constructive comments which led to an improved manuscript.

Conflicts of Interest: The authors declare no conflicts of interest.

References

- Li, S.; Wang, X.; Lu, Y.; Wang, J.; Yu, D.; Zhou, Z.; Wei, J.; Liu, L.; Liu, J.; Liu, F.; et al. Co-infections of *Klebsiella pneumoniae* and *Elizabethkingia miricola* in black-spotted frogs (*Pelophylax nigromaculatus*). *Microb. Pathog.* **2023**, *180*, 106150. [[CrossRef](#)] [[PubMed](#)]
- Kim, K.K.; Kim, M.K.; Lim, J.H.; Park, H.Y.; Lee, S.-T. Transfer of *Chryseobacterium meningosepticum* and *Chryseobacterium miricola* to *Elizabethkingia* gen. nov. as *Elizabethkingia meningoseptica* comb. nov. and *Elizabethkingia miricola* comb. nov. *Int. J. Syst. Evol. Microbiol.* **2005**, *55*, 1287–1293. [[CrossRef](#)]
- Zajmi, A.; Teo, J.; Yeo, C.C. Epidemiology and Characteristics of *Elizabethkingia* spp. Infections in Southeast Asia. *Microorganisms* **2022**, *10*, 882. [[CrossRef](#)] [[PubMed](#)]
- Hu, R.X.; Yuan, J.F.; Meng, Y.; Wang, Z.; Gu, Z.M. Pathogenic *Elizabethkingia miricola* Infection in Cultured Black-Spotted Frogs, China, 2016. *Emerg. Infect. Dis.* **2017**, *23*, 2055–2059. [[CrossRef](#)] [[PubMed](#)]
- Yang, S.; Si, C.; Mani, R.; Keller, J.; Hoenerhoff, M.J. Septicemia caused by an emerging pathogen, *Elizabethkingia miricola*, in a laboratory colony of African dwarf frogs (*Hymenochirus curtipes*). *Vet. Pathol.* **2023**, *60*, 394–401. [[CrossRef](#)] [[PubMed](#)]
- Wei, D.D.; Cheng, Y.; Xiao, S.Y.; Liao, W.Y.; Yu, Q.; Han, S.Y.; Huang, S.S.; Shi, J.G.; Xie, Z.S.; Li, P.F. Natural occurrences and characterization of *Elizabethkingia miricola* infection in cultured bullfrogs (*Rana catesbeiana*). *Front. Cell. Infect. Microbiol.* **2023**, *13*, 1094050. [[CrossRef](#)] [[PubMed](#)]
- Trimpert, J.; Eichhorn, I.; Vladimirova, D.; Haake, A.; Schink, A.K.; Klopfleisch, R.; Lubke-Becker, A. *Elizabethkingia miricola* infection in multiple anuran species. *Transbound. Emerg. Dis.* **2021**, *68*, 931–940. [[CrossRef](#)]
- Lei, X.P.; Yi, G.; Wang, K.Y.; OuYang, P.; Chen, D.F.; Huang, X.L.; Huang, C.; Lai, W.M.; Zhong, Z.J.; Huo, C.L.; et al. *Elizabethkingia miricola* infection in Chinese spiny frog (*Quasipaa spinosa*). *Transbound. Emerg. Dis.* **2019**, *66*, 1049–1053. [[CrossRef](#)]
- Hem, S.; Jarocki, V.M.; Baker, D.J.; Charles, I.G.; Drigo, B.; Aucote, S.; Donner, E.; Burnard, D.; Bauer, M.J.; Harris, P.N.A.; et al. Genomic analysis of *Elizabethkingia* species from aquatic environments: Evidence for potential clinical transmission. *Curr. Res. Microb. Sci.* **2022**, *3*, 100083. [[CrossRef](#)]
- Brestoff, J.R.; Artis, D. Commensal bacteria at the interface of host metabolism and the immune system. *Nat. Immunol.* **2013**, *14*, 676–684. [[CrossRef](#)]
- Glendinning, L.; Nausch, N.; Free, A.; Taylor, D.W.; Mutapi, F. The microbiota and helminths: Sharing the same niche in the human host. *Parasitology* **2014**, *141*, 1255–1271. [[CrossRef](#)] [[PubMed](#)]
- Manes, N.P.; Shulzhenko, N.; Nuccio, A.G.; Azeem, S.; Morgun, A.; Nita-Lazara, A. Multi-omics Comparative Analysis Reveals Multiple Layers of Host Signaling Pathway Regulation by the Gut Microbiota. *mSystems* **2017**, *2*, 22. [[CrossRef](#)] [[PubMed](#)]
- Bisht, V.; Nash, K.; Xu, Y.W.; Agarwal, P.; Bosch, S.; Gkoutos, G.V.; Acharjee, A. Integration of the Microbiome, Metabolome and Transcriptomics Data Identified Novel Metabolic Pathway Regulation in Colorectal Cancer. *Int. J. Mol. Sci.* **2021**, *22*, 5763. [[CrossRef](#)] [[PubMed](#)]
- Salinas, I.; Magadán, S. Omics in fish mucosal immunity. *Dev. Comp. Immunol.* **2017**, *75*, 99–108. [[CrossRef](#)] [[PubMed](#)]
- Li, X.; Yang, X.; Chang, L.; Wang, Z.; Wang, T.; Zhang, Z.; Bai, J.; Liang, R.; Niu, Q.; Zhang, H. Endoplasmic reticulum rather than mitochondria plays a major role in the neuronal apoptosis induced by polybrominated diphenyl ether-153. *Toxicol. Lett.* **2019**, *311*, 37–48. [[CrossRef](#)] [[PubMed](#)]
- Qiao, M.; Zhang, L.; Xu, C.; Huo, X.; Chang, J.; Su, J. Chitosan and anisodamine enhance the immersion immune efficacy of inactivated *Elizabethkingia miricola* vaccine in black spotted frogs. *Fish Shellfish Immunol.* **2022**, *130*, 93–102. [[CrossRef](#)] [[PubMed](#)]
- Forzán, M.J.; Jones, K.M.; Ariel, E.; Whittington, R.J.; Wood, J.; Markham, R.J.F.; Daoust, P.Y. Pathogenesis of Frog Virus 3 (*Ranavirus, Iridoviridae*) Infection in Wood Frogs (*Rana sylvatica*). *Vet. Pathol.* **2017**, *54*, 531–548. [[CrossRef](#)] [[PubMed](#)]

18. Guo, M.; Wu, F.; Hao, G.; Qi, Q.; Li, R.; Li, N.; Wei, L.; Chai, T. *Bacillus subtilis* Improves Immunity and Disease Resistance in Rabbits. *Front. Immunol.* **2017**, *8*, 354. [[CrossRef](#)]
19. Caporaso, J.G.; Kuczynski, J.; Stombaugh, J.; Bittinger, K.; Bushman, F.D.; Costello, E.K.; Fierer, N.; Peña, A.G.; Goodrich, J.K.; Gordon, J.I.; et al. QIIME allows analysis of high-throughput community sequencing data. *Nat. Methods* **2010**, *7*, 335–336. [[CrossRef](#)]
20. Edgar, R.C. Search and clustering orders of magnitude faster than BLAST. *Bioinformatics* **2010**, *26*, 2460–2461. [[CrossRef](#)]
21. DeSantis, T.Z.; Hugenholtz, P.; Larsen, N.; Rojas, M.; Brodie, E.L.; Keller, K.; Huber, T.; Dalevi, D.; Hu, P.; Andersen, G.L. Greengenes, a chimera-checked 16S rRNA gene database and workbench compatible with ARB. *Appl. Environ. Microbiol.* **2006**, *72*, 5069–5072. [[CrossRef](#)] [[PubMed](#)]
22. Ondov, B.D.; Bergman, N.H.; Phillippy, A.M. Interactive metagenomic visualization in a Web browser. *BMC Bioinform.* **2011**, *12*, 385. [[CrossRef](#)] [[PubMed](#)]
23. Segata, N.; Izard, J.; Waldron, L.; Gevers, D.; Miropolsky, L.; Garrett, W.S.; Huttenhower, C. Metagenomic biomarker discovery and explanation. *Genome Biol.* **2011**, *12*, R60. [[CrossRef](#)] [[PubMed](#)]
24. Langille, M.G.; Zaneveld, J.; Caporaso, J.G.; McDonald, D.; Knights, D.; Reyes, J.A.; Clemente, J.C.; Burkpile, D.E.; Vega Thurber, R.L.; Knight, R.; et al. Predictive functional profiling of microbial communities using 16S rRNA marker gene sequences. *Nat. Biotechnol.* **2013**, *31*, 814–821. [[CrossRef](#)] [[PubMed](#)]
25. Bai, L.; Li, H. Innate immune regulatory networks in hepatic lipid metabolism. *J. Mol. Med.* **2019**, *97*, 593–604. [[CrossRef](#)] [[PubMed](#)]
26. Kim, J.; Kim, G.-L.; Norambuena, J.; Boyd, J.M.; Parker, D. Impact of the pentose phosphate pathway on metabolism and pathogenesis of *Staphylococcus aureus*. *PLoS Pathog.* **2023**, *19*, e1011531. [[CrossRef](#)] [[PubMed](#)]
27. Su, J.; Li, S.; Chen, J.; Jian, C.; Hu, J.; Du, H.; Hai, H.; Wu, J.; Zeng, F.; Zhu, J.; et al. Glycerophospholipid metabolism is involved in rheumatoid arthritis pathogenesis by regulating the IL-6/JAK signaling pathway. *Biochem. Biophys. Res. Commun.* **2022**, *600*, 130–135. [[CrossRef](#)]
28. Branco, L.M.; Amaral, M.P.; Boekhoff, H.; de Lima, A.B.F.; Farias, I.S.; Lage, S.L.; Pereira, G.J.S.; Franklin, B.S.; Bortoluci, K.R. Lysosomal cathepsins act in concert with Gasdermin-D during NAIP/NLRC4-dependent IL-1 β secretion. *Cell Death Dis.* **2022**, *13*, 10. [[CrossRef](#)]
29. Hu, Y.; Li, A.; Xu, Y.; Jiang, B.; Lu, G.; Luo, X. Transcriptomic variation of locally-infected skin of *Epinephelus coioides* reveals the mucosal immune mechanism against *Cryptocaryon irritans*. *Fish Shellfish Immunol.* **2017**, *66*, 398–410. [[CrossRef](#)]
30. Kubica, P.; Lara-Velazquez, M.; Bam, M.; Siraj, S.; Ong, I.; Liu, P.; Priya, R.; Salamat, S.; Brutkiewicz, R.R.; Dey, M. MR1 overexpression correlates with poor clinical prognosis in glioma patients. *Neuro-Oncol. Adv.* **2021**, *3*, vdab034. [[CrossRef](#)]
31. Parks, W.C.; Wilson, C.L.; López-Boado, Y.S. Matrix metalloproteinases as modulators of inflammation and innate immunity. *Nat. Rev. Immunol.* **2004**, *4*, 617–629. [[CrossRef](#)] [[PubMed](#)]
32. Wiera, G.; Mozrzymas, J.W. Extracellular Metalloproteinases in the Plasticity of Excitatory and Inhibitory Synapses. *Cells* **2021**, *10*, 2055. [[CrossRef](#)] [[PubMed](#)]
33. Graves, A.M.Z. Investigating the Roles of HLA-DO in the Immune Response in Humans and Mice. Ph.D. Thesis, School of Graduate Studies, Rutgers University, New Brunswick, NJ, USA, 2021.
34. Fan, T.-J.; Han, L.-H.; Cong, R.-S.; Liang, J. Caspase Family Proteases and Apoptosis. *Acta Biochim. Biophys. Sin.* **2005**, *37*, 719–727. [[CrossRef](#)] [[PubMed](#)]
35. Li, Y.-F.; Yi, P.; Wang, Y.-L.; Wu, X.-J.; Yang, F.; Ma, H.-N.; Tan, M.-S. Function of NOD-like receptor protein 1 inflammasome in traumatic central nervous system injury. *Zhongguo Gu Shang = China J. Orthop. Traumatol.* **2021**, *34*, 1058–1064. [[CrossRef](#)]
36. Liu, Y.; Xing, L.H.; Li, F.X.; Wang, N.; Ma, Y.Z.; Li, J.W.; Wu, Y.J.; Liang, J.; Lei, Y.X.; Wang, X.Y.; et al. Mixed lineage kinase-like protein protects against *Clostridium perfringens* infection by enhancing NLRP3 inflammasome-extracellular traps axis. *iScience* **2022**, *25*, 105121. [[CrossRef](#)]
37. Lee, E.J.; Napier, R.J.; Vance, E.E.; Lashley, S.J.; Truax, A.D.; Ting, J.P.; Rosenzweig, H.L. The innate immune receptor Nlrp12 suppresses autoimmunity to the retina. *J. Neuroinflamm.* **2022**, *19*, 12. [[CrossRef](#)]
38. Ding, J.D.; Kelly, U.; Landowski, M.; Toomey, C.B.; Groelle, M.; Miller, C.; Smith, S.G.; Klingeborn, M.; Singhapricha, T.; Jiang, H.X.; et al. Expression of Human Complement Factor H Prevents Age-Related Macular Degeneration-Like Retina Damage and Kidney Abnormalities in Aged *Cfh* Knockout Mice. *Am. J. Pathol.* **2015**, *185*, 29–42. [[CrossRef](#)]
39. Vakhrusheva, T.V.; Grigorieva, D.V.; Gorudko, I.V.; Sokolov, A.V.; Kostevich, V.A.; Lazarev, V.N.; Vasilyev, V.B.; Cherenkevich, S.N.; Panasenko, O.M. Enzymatic and bactericidal activity of myeloperoxidase in conditions of halogenative stress. *Biochem. Cell Biol.* **2018**, *96*, 580–591. [[CrossRef](#)]
40. Canney, M.; Clark, E.G.; Hiremath, S. Biomarkers in acute kidney injury: On the cusp of a new era? *J. Clin. Investig.* **2023**, *133*, 13. [[CrossRef](#)]
41. Antonia, A.L.; Gibbs, K.D.; Trahair, E.D.; Pittman, K.J.; Martin, A.T.; Schott, B.H.; Smith, J.S.; Rajagopal, S.; Thompson, J.W.; Reinhardt, R.L.; et al. Pathogen Evasion of Chemokine Response Through Suppression of CXCL10. *Front. Cell. Infect. Microbiol.* **2019**, *9*, 280. [[CrossRef](#)]
42. Peachey, L.E.; Jenkins, T.P.; Cantacessi, C. This Gut Ain't Big Enough for Both of Us. Or Is It? Helminth–Microbiota Interactions in Veterinary Species. *Trends Parasitol.* **2017**, *33*, 619–632. [[CrossRef](#)] [[PubMed](#)]

43. Wei, D.; Xiao, S.; Liao, W.; Yu, Q.; Han, S.; Shi, J.; He, J.; Li, P. The occurrence of *Morganella morganii* caused large death in cultured American bullfrog (*Rana catesbeiana*). *Aquaculture* **2023**, *568*, 739343. [[CrossRef](#)]
44. Ramkumar, R.; Ravi, M.; Jayaseelan, C.; Rahuman, A.A.; Anandhi, M.; Rajthilak, C.; Perumal, P. Description of *Providencia vermicola* isolated from diseased Indian major carp, *Labeo rohita* (Hamilton, 1822). *Aquaculture* **2014**, *420*, 193–197. [[CrossRef](#)]
45. Camus, A.C.; Hawke, J.P. *Providencia rettgeri*-associated Septicemia and Meningoencephalitis in Juvenile Farmed American Alligators *Alligator mississippiensis*. *J. Aquat. Anim. Health* **2002**, *14*, 149–153. [[CrossRef](#)]
46. Yang, P.K.; Zheng, Y.Z.; Aweya, J.J.; Zou, X.H.; Lin, M.; Liu, Y.Q.; Zhang, Z.X.; Sun, Y.J.; Wang, H.J. iTRAQ-based comparative proteomic analysis of the *Lithobates catesbeianus* bullfrog spleen following challenge with *Citrobacter freundii*. *Aquac. Rep.* **2022**, *23*, 101037. [[CrossRef](#)]
47. Ramakrishna, C.; Kujawski, M.; Chug, H.; Li, L.; Mazmanian, S.K.; Cantin, E.M. *Bacteroides fragilis* polysaccharide A induces IL-10 secreting B and T cells that prevent viral encephalitis. *Nat. Commun.* **2019**, *10*, 2153. [[CrossRef](#)] [[PubMed](#)]
48. Arnolds, K.L.; Yamada, E.; Neff, C.P.; Schneider, J.M.; Palmer, B.E.; Lozupone, C.A. Disruption of Genes Encoding Putative Zwitterionic Capsular Polysaccharides of Diverse Intestinal *Bacteroides* Reduces the Induction of Host Anti-Inflammatory Factors. *Microb. Ecol.* **2023**, *85*, 1620–1629. [[CrossRef](#)]

Disclaimer/Publisher’s Note: The statements, opinions and data contained in all publications are solely those of the individual author(s) and contributor(s) and not of MDPI and/or the editor(s). MDPI and/or the editor(s) disclaim responsibility for any injury to people or property resulting from any ideas, methods, instructions or products referred to in the content.